DOI 10.1007/s10946-024-10183-9
Journal of Russian Laser Research, Volume 45, Number 1, January, 2024

THE PHYSICAL TRANSIENT SPECTRUM AND SQUEEZING OF A THREE-LEVEL ATOM INTERACTING WITH TWO-MODE FIELD IN FINITE PAIR COHERENT STATE IN THE PRESENCE OF A CLASSICAL EXTERNAL FIELD

A.-S. F. Obada,[1] E. M. Khalil,[2] S. Sanad,[3] and H. F. Habeba[4*]

[1] *Mathematics Department, Faculty of Science, Al-Azhar University Nasr City 11884, Cairo, Egypt*

[2] *Department of Mathematics, College of Science, P.O. Box 11099, Taif University Taif 21944, Saudi Arabia*

[3] *Mathematics Department, Faculty of Science (Girls Branch), Al-Azhar University Nasr City 11884, Cairo, Egypt*

[4] *Department of Mathematics and Computer Science, Faculty of Science, Menoufia University Shebin Elkom 32511, Egypt*

*Corresponding author e-mail: halahapepa@yahoo.com

Abstract

We investigate effects of a classical external field and the initial state of the field on the nonlinear interaction of a Λ-type three-level atom with the two-mode field through the Raman type interaction. Appropriate canonical transforms are performed for atomic states. The analytic solution to the model is obtained, using the Schrödinger differential equation. The wave function is obtained under specific initial conditions of the atom and field. The effect of a classical external field and the initial state of the field on the population occupations, the squeezing phenomenon, and the atomic emission spectrum are studied. The collapse–revival phenomena are affected by the presence of the classical field. Increasing the activation of the role of the initial state of the field improves the phenomena of collapses and revivals. The squeezing intervals decrease with increase in the classical field effect. The squeezing intervals increase with decrease of the parameter of the initial state of the field. The maximum values of the emission spectrum are improved after taking into account the classical field. In addition, the peaks significantly decrease after reducing the influence of both the bandwidth of the filter and the interaction time.

Keywords: finite pair coherent state, external classical field, squeezing phenomena, physical transient spectrum.

1. Introduction

The interaction between the atom and the quantum field has been extensively studied, due to its applications in a number of different fields, such as the lasing without inversion [1], laser cooling [2], and electromagnetically-induced transparency [3, 4]. There are some models that describe such interaction, the most important of which is the Jaynes–Cummings model (JCM) [5]. It has been experimentally implemented and solved exactly in the rotating wave approximation (RWA) and has been subjected to

Manuscript submitted by the authors in English on November 2, 2023.

many theoretical investigations [6–8]. There are many generalizations of this model, such as multilevel atom [9–13], multi-photon transitions [14], and multi-mode field [15, 16].

The effect of an external classical field (ECF) on some quantum properties, such as degree of the entanglement, the squeezing phenomenon and the phenomenon of revivals and collapses (RCP) has been studied in different models. The effect of the ECF on the squeezing phenomenon, the entanglement, and RCP has been studied in the JCM [17]. The influence of damping and ECF on the JCM has been discussed in [18]. Also, generating multipartite entanglement in N two-level atoms interacting with a quantized field and external classical fields was realized [19]. The effect of ECF and a nonlinear medium on the interaction between an electromagnetic field and a two-level atom has been studied [20]. The influence of ECF on the squeezing phenomena and the geometric phase of the interaction of two two-level atoms and N-level atom has been studied [21]. The effect of ECF and damping on the entropy squeezing and the nonlocal correlation between a nonlinear quantum system and two-level atom has been examined [22]. The analytical solution for a quantized cavity field interacting with a two-qubit system in the presence of two types of external fields has been derived; also, the quantum coherence and the entanglement have been discussed [23].

On the other hand, the physical transient spectrum received a lot of attention over recent years, because it contains information on the atom–field interaction. The physical transient spectrum of a three-level atom in $\vee$-configuration, where two upper levels are coupled by a classical field, has been studied [24]. The effects of a broadband squeezed vacuum on three-level atoms at different configurations have been investigated [25–27]. Also, the effect of the mean photon numbers and detuning parameter on the emission and absorption spectra have been analyzed for a Λ-type three-level atom interacting with a two-mode cavity field [28]. The effect of the photon multiplicities, detuning parameter, and mean photon number on the emission spectrum have been studied for a multi-photon Ξ-type three-level atom interacting with one-mode cavity field [29]. The analytical form of the emission spectrum has been calculated, using the dressed state of the interaction of a three-level atom with a multi-photon single-mode cavity field [30].

The aim of this paper is to study the effect of ECF on Λ-type three-level atom–field interaction, by analyzing the atomic-level occupations and the squeezing phenomena and using the finite pair coherent state. Also, we study the physical transient spectrum.

This paper is organized as follows.

In the next section, we introduce the formulation and analytical relation of the problem. In Sec. 3, we study the atomic-level occupations. In Sec. 4, we investigate the squeezing phenomena. Then, the physical transient spectrum is analyzed in Sec. 5. Finally, some concluding remarks are given in Sec. 6.

2. The Formulation of the Problem

In Fig. 1, we show the system Hamiltonian describing the interaction between a three-level atom in Λ-configuration and two correlated modes in the presence of classical external field. There is no dissipative processes in this system like the spontaneous emission, dephasing of transitions, etc. Assuming $\hbar = 1$, this Hamiltonian can be written as follows [31]:

$$\hat{H} = \hat{H}_0 + \hat{H}_1 + \hat{H}_2, \tag{1}$$

where

$$\hat{H}_0 = \frac{\omega}{2}(\hat{a}^\dagger\hat{a} - \hat{b}^\dagger\hat{b}) + \omega_e|e\rangle\langle e| + \omega_i|i\rangle\langle i| + \omega_g|g\rangle\langle g|, \quad (2)$$

$$\hat{H}_1 = i\Omega(\hat{a}^\dagger\hat{b} + \hat{a}\hat{b}^\dagger)(|e\rangle\langle g| - |g\rangle\langle e|) + i\Omega(\hat{a}^\dagger\hat{b} + \hat{a}\hat{b}^\dagger)(|e\rangle\langle i| - |i\rangle\langle e|), \quad (3)$$

and

$$\hat{H}_2 = \tau(|2\rangle\langle 3| + |3\rangle\langle 2|). \quad (4)$$

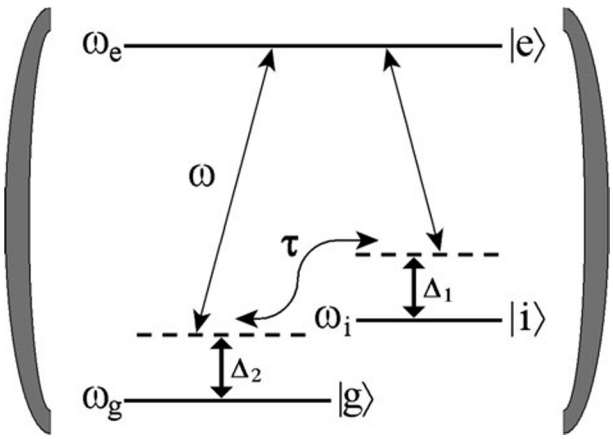

Fig. 1. A sketch of the three-level atom in the Λ-configuration located inside a cavity field with an external classical field.

Also, in Eq. (1), ω represents the field frequency, and ω_β with $\beta \in \{e, i, g\}$ are the frequencies of the atomic levels, with $\omega_g < \omega_i < \omega_e$; operators $\hat{a}$ and $\hat{b}$ are the boson operators for the field, satisfying the commutation relations $[\hat{a}, \hat{b}] = 0$, $[\hat{a}, \hat{a}^\dagger] = \hat{I}$, and $[\hat{b}, \hat{b}^\dagger] = \hat{I}$. Then, operators $|l\rangle\langle m|$; $l, m \in \{e, i, g\}$ satisfy the commutation relations $[|l\rangle\langle m||u\rangle\langle o|] = |l\rangle\langle o|\delta_{mu} - |u\rangle\langle m|\delta_{lo}$, Ω represents the quantized field coupling parameter, and τ is the ECF coupling parameter.

In order to solve Hamiltonian (1), we introduce the following transform:

$$\begin{pmatrix} |e\rangle \\ |i\rangle \\ |g\rangle \end{pmatrix} = \begin{pmatrix} 1 & 0 & 0 \\ 0 & \cos(\vartheta) & \sin(\vartheta) \\ 0 & -\sin(\vartheta) & \cos(\vartheta) \end{pmatrix} \begin{pmatrix} |1\rangle \\ |2\rangle \\ |3\rangle \end{pmatrix}, \quad (5)$$

where $\vartheta = \frac{1}{2}\arctan\left(\frac{2\tau}{\omega_g - \omega_i}\right)$.

Using this transform and applying RWA to Hamiltonian (1), we obtain the transformed Hamiltonian as follows:

$$\hat{H}_{\text{tran}} = \hat{H}_1 + \hat{H}_2, \quad (6)$$

where

$$\hat{H}_1 = \frac{\omega}{2}(\hat{n}_a - \hat{n}_b) + \omega_e|1\rangle\langle 1| + \bar{\Omega}_i|2\rangle\langle 2| + \bar{\Omega}_g|3\rangle\langle 3|, \quad (7)$$

$$\hat{H}_2 = i\mu_1(\hat{a}\hat{b}^\dagger|1\rangle\langle 2| - \hat{a}^\dagger\hat{b}|2\rangle\langle 1|) + i\mu_2(\hat{a}\hat{b}^\dagger|1\rangle\langle 3| - \hat{a}^\dagger\hat{b}|3\rangle\langle 1|), \quad (8)$$

with

$$\hat{n}_a = \hat{a}^\dagger\hat{a}, \hat{n}_b = \hat{b}^\dagger\hat{b}, \quad (9)$$

$$\bar{\Omega}_i = \omega_i\cos^2(\vartheta) + \omega_g\sin^2(\vartheta) - \tau\sin(2\vartheta), \quad (10)$$

$$\bar{\Omega}_g = \omega_g\cos^2(\vartheta) + \omega_i\sin^2(\vartheta) + \tau\sin(2\vartheta), \quad (11)$$

$$\mu_1 = \Omega[\cos(\vartheta) - \sin(\vartheta)], \quad (12)$$

$$\mu_2 = \Omega[\cos(\vartheta) + \sin(\vartheta)]. \quad (13)$$

Now, we need to find the exact solution of Hamiltonian (6); so we look for the interaction picture of the Hamiltonian in the following form:

$$\hat{H}_{\text{int}} = i\mu_1(\hat{a}\hat{b}^\dagger e^{i\Delta_1 t}|1\rangle\langle 2| - \hat{a}^\dagger\hat{b}e^{-i\Delta_1 t}|2\rangle\langle 1|) + i\mu_2(\hat{a}\hat{b}^\dagger e^{-i\Delta_2 t}|1\rangle\langle 3| - \hat{a}^\dagger\hat{b}e^{i\Delta_2 t}|3\rangle\langle 1|), \quad (14)$$

where the detuning parameters Δ_α; $\alpha = 1, 2$ read

$$\Delta_1 = -\omega - (\bar{\Omega}_i - \omega_e), \tag{15}$$
$$\Delta_2 = \omega - (\omega_e - \bar{\Omega}_g). \tag{16}$$

The initial state $|u_{\rm AF}(0)\rangle$ of the atom–field system reads

$$|u_{\rm AF}(0)\rangle = |u_A(0)\rangle \otimes |u_F(0)\rangle, \tag{17}$$

where the initial state of the atom $|u_A(0)\rangle = |1\rangle$ is the upper-most state, the initial state of the field $|u_F(0)\rangle = |\xi, q\rangle$, and the initial state $|\xi, q\rangle$ represents the finite pair coherent state; it is [32]

$$|\xi, q\rangle = N_q \sum_{n=0}^{q} \xi^n \sqrt{\frac{(q-n)!}{q!n!}} |q-n, n\rangle, \tag{18}$$

with

$$N_q = \left[\sum_{n=0}^{q} |\xi|^{2n} \frac{(q-n)!}{q!n!}\right]^{-1/2}, \tag{19}$$

where q is a positive integer, and ξ may be a complex number.

The exact solution of (14) at $t > 0$ may be considered in the following form:

$$|u(t)\rangle = \sum_{n=0}^{q} [A_1(n,t)|1, q-n-1, n+1\rangle + A_2(n,t)|2, q-n, n\rangle + A_3(n,t)|3, q-n, n\rangle], \tag{20}$$

where $A_i(n,t)$; $i = 1, 2, 3$ are the probability amplitudes, which satisfy $\sum\limits_{i=1}^{3} |A_i(n,t)|^2 = 1$. In view the Schrödinger equation, we obtain the following system of differential equations:

$$i\frac{d}{dt}A_1(n,t) = \Pi_1 e^{i\Delta_1 t} A_2(n,t) + \Pi_2 e^{-i\Delta_2 t} A_3(n,t), \tag{21}$$
$$i\frac{d}{dt}A_2(n,t) = -\Pi_1 e^{-i\Delta_1 t} A_1(n,t), \tag{22}$$
$$i\frac{d}{dt}A_3(n,t) = -\Pi_2 e^{i\Delta_2 t} A_1(n,t), \tag{23}$$

where

$$\Pi_j = i\mu_j \sqrt{n+1}\sqrt{q-n}; \qquad j = 1, 2. \tag{24}$$

If we assume $A_2(n,t) = e^{i\varepsilon t}$ in Eq. (21) and insert it in Eq. (23), we obtain the cubic equation for ε; it reads

$$\varepsilon^3 + \iota_1 \varepsilon^2 + \iota_2 \varepsilon + \iota_3 = 0, \tag{25}$$

where

$$\iota_1 = 2\Delta_1 + \Delta_2, \tag{26}$$
$$\iota_2 = \Delta_1^2 + \Delta_1\Delta_2 + \Pi_1^2 + \Pi_2^2, \tag{27}$$
$$\iota_3 = \Pi_1^2(\Delta_1 + \Delta_2). \tag{28}$$

The solution of this equation is

$$\varepsilon_j = -\frac{1}{3}\iota_1 + \frac{2}{3}\sqrt{\iota_1^2 - 3\iota_2}\cos\left[\varkappa + \frac{2}{3}(j-1)\pi\right]; \qquad j = 1,2,3, \tag{29}$$

where

$$\varkappa = \frac{1}{3}\cos^{-1}\left[\frac{-2\iota_1^3 + 9\iota_1\iota_2 - 27\iota_3}{2(-3\iota_2 + \iota_1^2)^{3/2}}\right]. \tag{30}$$

When $A_2(n,t)$ is taken as a linear combination of $e^{i\varepsilon_j t}$,

$$A_2(n,t) = \Pi_1 \sum_{j=1}^{3} b_j e^{i\varepsilon_j t}, \tag{31}$$

after inserting it in the differential equations (21)–(23), we arrive at $A_i(n,t)$ as follows:

$$A_1(n,t) = \sum_{j=1}^{3} b_j \varepsilon_j e^{i(\varepsilon_j + \Delta_1)t}, \tag{32}$$

$$A_2(n,t) = \Pi_1 \sum_{j=1}^{3} b_j e^{i\varepsilon_j t}, \tag{33}$$

$$A_3(n,t) = \frac{-1}{\Pi_2}\sum_{j=1}^{3} b_j[\varepsilon_j(\varepsilon_j + \Delta_1) + \Pi_1^2]e^{i(\varepsilon_j + \Delta_1 + \Delta_2)t}. \tag{34}$$

Coefficients b_j; $j = 1,2,3$ are determined from the initial condition $|u_{\rm AF}(0)\rangle$ (17), which amount to $A_1(n,0) = N_q \sum\limits_{n=0}^{q} \xi^n \sqrt{\dfrac{(q-n)!}{q!n!}}$ and $A_2(n,0) = 0 = A_3(n,0)$.

Now, we can obtain the wave function of Hamiltonian (1) at $t > 0$ as follows:

$$|\Phi(t)\rangle = \sum_{n=0}^{q}[Y_1(n,t)|e, q-n-1, n+1\rangle + Y_2(n,t)|i, q-n, n\rangle + Y_3(n,t)|g, q-n, n\rangle], \tag{35}$$

where

$$Y_1(n,t) = A_1(n,t), \tag{36}$$

$$Y_2(n,t) = A_2(n,t)\cos(\varepsilon) + A_3(n,t)\sin(\varepsilon), \tag{37}$$

$$Y_3(n,t) = -A_2(n,t)\sin(\varepsilon) + A_3(n,t)\cos(\varepsilon). \tag{38}$$

Then, the reduced atomic density matrix $\hat{\wp}_{\rm atom}(t)$ reads

$$\hat{\wp}_{\rm atom}(t) = {\rm Tr}_{\rm field}\,|\Phi(t)\rangle\langle\Phi(t)|, \qquad \hat{\wp}_{\rm atom}(t) = \begin{pmatrix} \wp_{ee}(t) & \wp_{ei}(t) & \wp_{eg}(t) \\ \wp_{ie}(t) & \wp_{ii}(t) & \wp_{ig}(t) \\ \wp_{ge}(t) & \wp_{gi}(t) & \wp_{gg}(t) \end{pmatrix}, \tag{39}$$

where

$$\wp_{ee}(t) = \sum_{n=0}^{q} |Y_1(n,t)|^2, \qquad \wp_{ii}(t) = \sum_{n=0}^{q} |Y_2(n,t)|^2, \qquad \wp_{gg}(t) = \sum_{n=0}^{q} |Y_3(n,t)|^2, \tag{40}$$

$$\wp_{ei}(t) = \sum_{n=0}^{q} Y_1(n,t) Y_2^*(n+1,t) = \wp_{ie}^*(t), \tag{41}$$

$$\wp_{eg}(t) = \sum_{n=0}^{q} Y_1(n,t) Y_3^*(n+1,t) = \wp_{ge}^*(t), \tag{42}$$

$$\wp_{ig}(t) = \sum_{n=0}^{q} Y_2(n,t) Y_3^*(n,t) = \wp_{gi}^*(t). \tag{43}$$

In what follows, we discuss some nonclassical properties of the system under study, such as the atomic level occupations, squeezing phenomena, and the atomic emission spectrum.

3. The Atomic Level Occupations

In this section, we use the atomic level occupations $\rho_{ee}(t)$, $\rho_{ii}(t)$, and $\rho_{gg}(t)$ to obtain the collapse and revival intervals during the interaction period. Undoubtedly, the phenomena of collapses and revivals have a great importance in quantum information. Previous studies also confirmed that determination of periods of collapses and revivals depends on the Rabi frequency [33].

We investigate the effect of classical field on the atomic level occupations with two values for the parameter ξ. First, the classical field effect ($\tau = 0$) is neglected, and a small value for the parameter $\xi = 3$ is considered. In Fig. 2 a, we confirm the congruence of the occupation $\rho_{gg}(t)$ and $\rho_{ii}(t)$ and show chaotic oscillations. The $\rho_{ee}(t)$ occupation fluctuates with a large amplitude and ranging between 0.3 and 1. In the three level occupations, the phenomenon of collapses and revivals does not occur during the interaction period. The phenomenon of collapses and revivals is generated after increasing the parameter ξ to 20. Moreover, the amplitudes of the oscillations decrease, and successive periods of revival are formed; see Fig. 2 b. The three values of occupatrion values $\rho_{ee}(t)$, $\rho_{ii}(t)$, and $\rho_{gg}(t)$ appear different after taking into account the external field. The amplitudes of the oscillations improve and an exchange of roles is generated for the $\rho_{ii}(t)$ and $\rho_{gg}(t)$ levels; see Fig. 2 c. When $\xi = 20$ is seated, the exchange of oscillations between the $\rho_{ii}(t)$ and $\rho_{gg}(t)$ levels is more pronounced. The collapse periods in the absence of the classical field is erased after adding the classical field to the interaction; see Fig. 1 d. When the parameter ξ is small, the occupation numbers improve greatly with increase in the intensity of the oscillations. The oscillations decrease, when the parameter ξ is taken large; see Figs. 2 e, f.

4. The Squeezing Phenomena

In this section, we study the squeezing phenomenon, which is considered as one of the nonclassical phenomena in quantum optics, using the entropy and the variance squeezing.

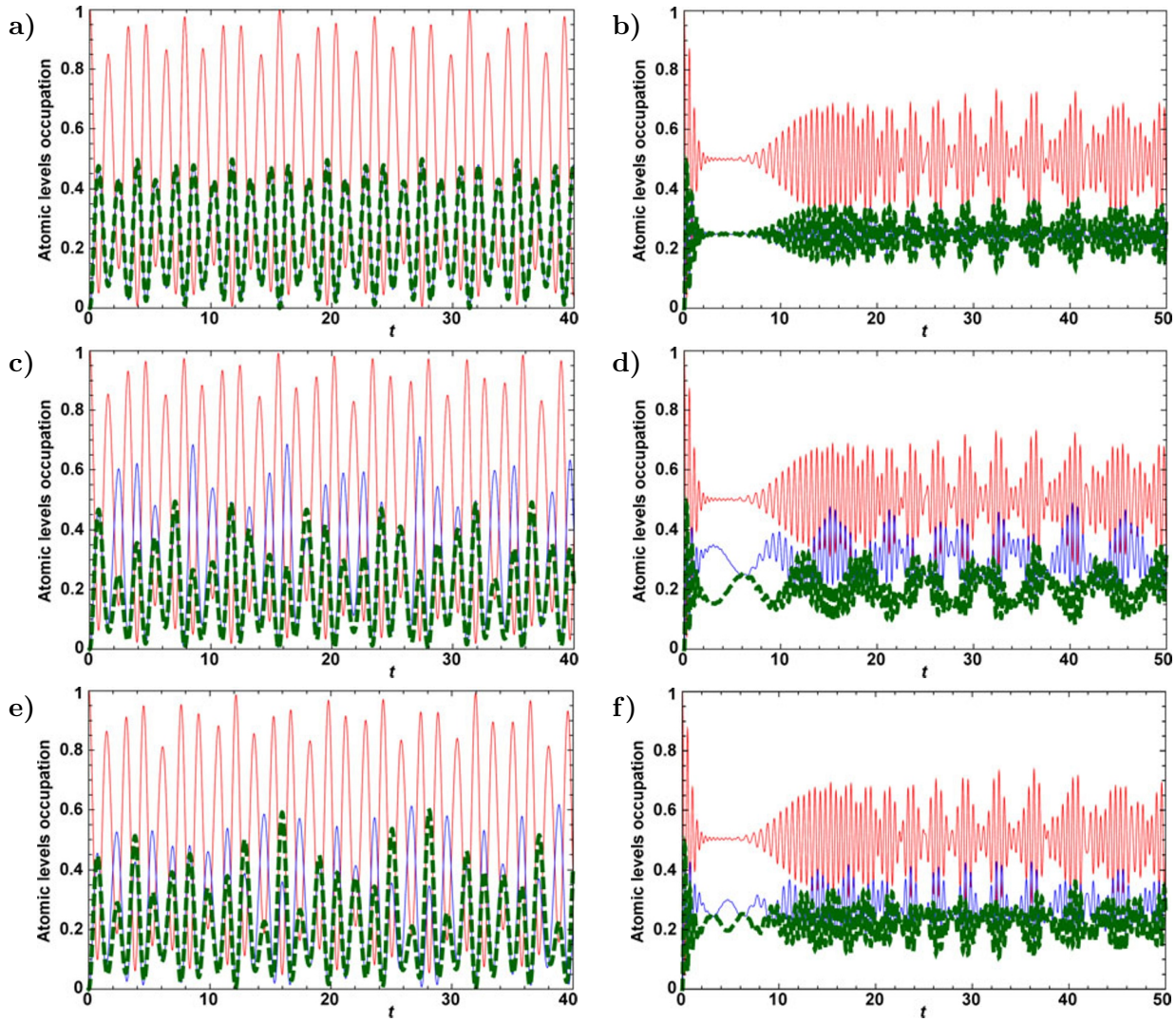

Fig. 2. The time evolution of the atomic level occupations as a function of the scaled time t; here, $q = 50$, $\Omega = 0.2$, $\omega_e = 1$, $\omega_i = 0.6$, $\omega_g = 0.4$, $\omega = 0.5$, and $\xi = 3$ (a, c, e) and $\xi = 20$ (b, d, f). Here, $\rho_{ee}(t)$ is shown by the red curve, $\rho_{ii}(t)$, by the blue curve, and $\rho_{gg}(t)$, by the green curve at $\tau = 0$ (a, b), $\tau = 0.5$ (c, d), and at $\tau = 1$ (e, f).

4.1. The Entropy Squeezing

The entropic uncertainty relation for $(d+1)$ complementary observables is described by the following inequality [34–36]:

$$\sum_{\sigma=1}^{d+1} H(\hat{L}_\sigma) \geq d \ln \left[\frac{1}{2}(d+1)\right]. \tag{44}$$

This inequality is achieved for a prime d-dimensional Hilbert space only.

The Shannon information entropy $H(\hat{L}_\sigma)$ is defined as follows:

$$H(\hat{L}_\sigma) = -\sum_{\alpha=1}^{d} G_\alpha(\hat{L}_\sigma) \ln G_\alpha(\hat{L}_\sigma); \qquad \sigma = x, y, z, \tag{45}$$

where $G_\alpha(\hat{L}_\sigma)$ represents the probability distribution for n possible outcomes of measurements of the operator $\hat{L}_\sigma$.

In the case of the three-level atom, $G_\alpha(\hat{L}_\sigma)$ are calculated as [35–37]

$$G_1(\hat{L}_x) = \frac{1}{2}(\wp_{ee}(t) - 2\mathrm{Re}\,[\wp_{eg}(t)] + \wp_{gg}(t)), \tag{46}$$

$$G_2(\hat{L}_x) = \frac{1}{4}\wp_{ee}(t) + \frac{1}{\sqrt{2}}\mathrm{Re}\,[\wp_{ei}(t)] + \frac{1}{2}\wp_{ii}(t) + \frac{1}{2}\mathrm{Re}\,[\wp_{eg}(t)] + \frac{1}{\sqrt{2}}\mathrm{Re}\,[\wp_{ig}(t)] + \frac{1}{4}\wp_{gg}(t), \tag{47}$$

$$G_3(\hat{L}_x) = \frac{1}{4}\wp_{ee}(t) - \frac{1}{\sqrt{2}}\mathrm{Re}\,[\wp_{ei}(t)] + \frac{1}{2}\wp_{ii}(t) + \frac{1}{2}\mathrm{Re}\,[\wp_{eg}(t)] - \frac{1}{\sqrt{2}}\mathrm{Re}\,[\wp_{ig}(t)] + \frac{1}{4}\wp_{gg}(t). \tag{48}$$

$$G_1(\hat{L}_y) = \frac{1}{2}\{\wp_{ee}(t) + \wp_{gg}(t) + 2\mathrm{Re}\,[\wp_{eg}(t)]\}, \tag{49}$$

$$G_2(\hat{L}_y) = \frac{1}{4}\wp_{ee}(t) + \frac{1}{2}\wp_{ii}(t) + \frac{1}{4}\wp_{gg}(t) + \frac{1}{\sqrt{2}}\mathrm{Im}\,[\wp_{ei}(t)] - \frac{1}{2}\mathrm{Re}\,[\wp_{eg}(t)] + \frac{1}{\sqrt{2}}\mathrm{Im}\,[\wp_{ig}(t)], \tag{50}$$

$$G_3(\hat{L}_y) = \frac{1}{4}\wp_{ee}(t) + \frac{1}{2}\wp_{ii}(t) - \frac{1}{\sqrt{2}}\mathrm{Im}\,[\wp_{ei}(t)] - \frac{1}{2}\mathrm{Re}\,[\wp_{eg}(t)] - \frac{1}{\sqrt{2}}\mathrm{Im}\,[\wp_{ig}(t)] + \frac{1}{4}\wp_{gg}(t). \tag{51}$$

$$G_1(\hat{L}_z) = \wp_{ee}(t), \qquad G_2(\hat{L}_z) = \wp_{ii}(t), \qquad G_3(\hat{L}_z) = \wp_{gg}(t). \tag{52}$$

In view of inequality (44), $H(\hat{L}_\sigma)$ satisfies the following relation:

$$H(\hat{L}_x) + H(\hat{L}_y) + H(\hat{L}_z) \geq 3\ln 2. \tag{53}$$

When $\delta(\hat{L}_\sigma) = \exp[H(\hat{L}_\beta)]$, we obtain

$$\delta H(\hat{L}_x)\delta H(\hat{L}_y)\delta H(\hat{L}_z) \geq 8. \tag{54}$$

Then the fluctuation in $\hat{L}_\sigma$; $\sigma = x, y$ represents squeezing, if $H(\hat{L}_\sigma)$ satisfies the following condition:

$$E(\hat{L}_\sigma) = \left[\delta H(\hat{L}_\sigma) - \frac{2\sqrt{2}}{\sqrt{|\delta H(\hat{L}_z)|}}\right] < 0; \qquad \sigma = x, y. \tag{55}$$

We devote this part to the study of the effect of classical field and the parameter ξ on the squeezing intervals, using the conditions mentioned above in the level occupations. First, the classical field effect ($\tau = 0$) is neglected and a small value for the parameter $\xi = 3$ is considered. In Fig. 3 a, we show two curves of $E(\hat{L}_x)$ and $E(\hat{L}_y)$, which randomly fluctuate and approach negative values in the most of the interaction period. The squeezing is achieved in the quadrature $E(\hat{L}_x)$, while it is not achieved in the quadrature $E(\hat{L}_y)$. The squeezing intervals slightly improve after increase in the parameter ξ to 20. Moreover, the oscillation intensities of the curves increase, and the squeezing is not achieved in most of the interaction period; see Fig. 3 b. The squeezing in both quadratures $E(\hat{L}_x)$ and $E(\hat{L}_y)$ is interchangeably exhibited, when the parameter ξ is small; see Fig. 3 c. In Fig. 3, we show the regularity of the curves; the squeezing intervals are erased after increasing ξ to 20; see Fig. 3 d. In Fig. 3 e, f, we show that the squeezing intervals significantly decrease with increasing influence of the classical field, whether in the case of small or large ξ.

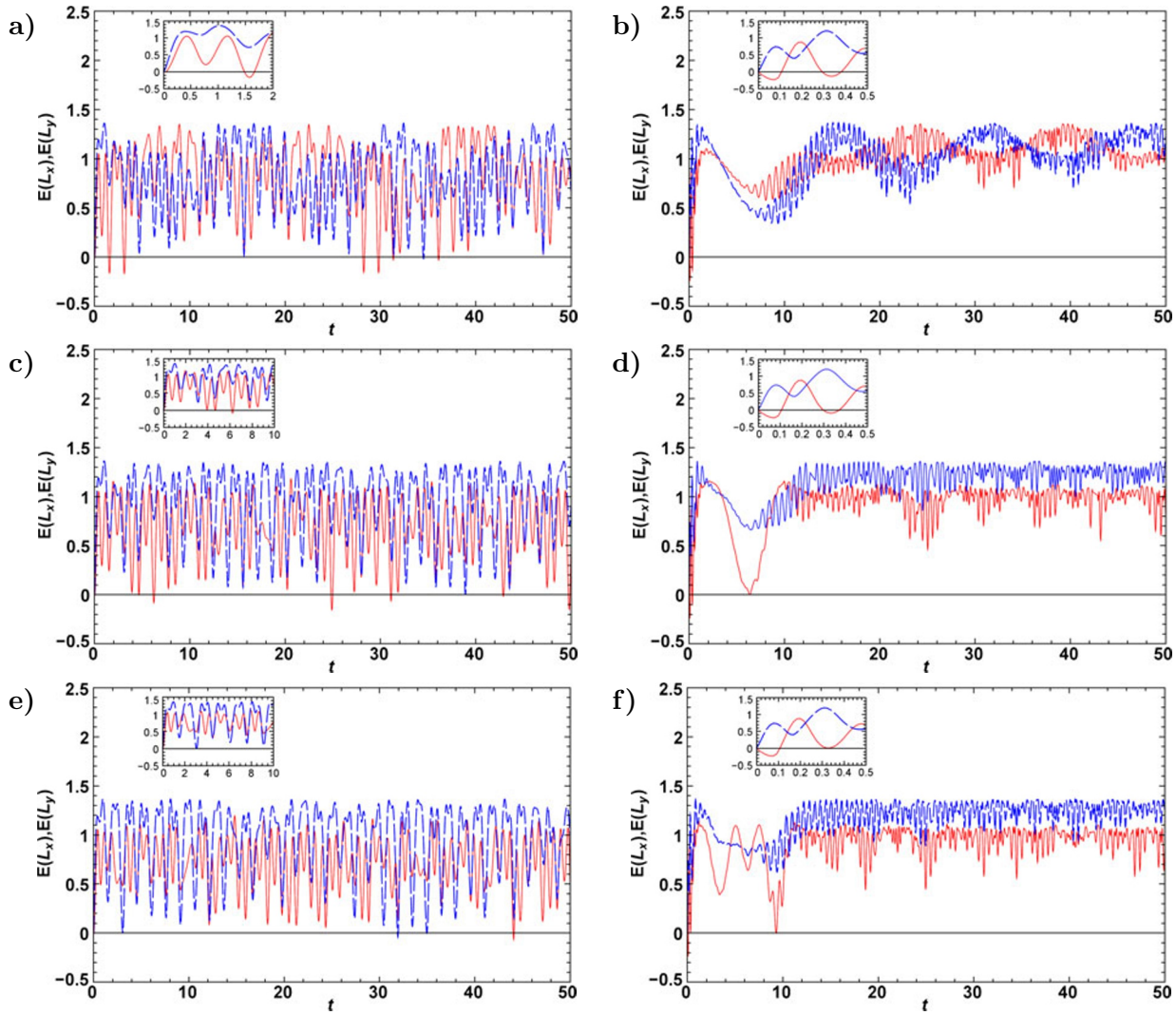

Fig. 3. The time evolution of the entropy squeezing components $E(\hat{L}_x)$ (red curves) and $E(\hat{L}_y)$ (blue curves) as functions of scaled time t. The parameters are the same as in Fig. 2.

4.2. Squeezing in the Atomic Variables

In this section, we study the squeezing phenomena of the atomic variables – the variance squeezing. The uncertainty relation for any three-level atom reads [38]

$$\triangle \hat{l}_x \triangle \hat{l}_y \geqslant \frac{1}{2}\left|\langle \hat{l}_z \rangle\right|, \tag{56}$$

where $\hat{l}_x$, $\hat{l}_y$, and $\hat{l}_z$ satisfy the relation $[\hat{l}_x, \hat{L}_y] = i\hat{l}_z$.

The expectation values of $\hat{l}_x$, $\hat{l}_y$, and $\hat{l}_z$ for the three-level atom are

$$\langle \hat{l}_x \rangle = \frac{1}{\sqrt{2}}(\wp_{ei}(t) + \wp_{ie}(t) + \wp_{ig}(t) + \wp_{gi}(t)), \tag{57}$$

$$\langle \hat{l}_y \rangle = \frac{i}{\sqrt{2}}(-\wp_{ei}(t) + \wp_{ie}(t) - \wp_{ig}(t) + \wp_{gi}(t)), \tag{58}$$

$$\langle \hat{l}_z \rangle = \wp_{ee}(t) - \wp_{gg}(t). \tag{59}$$

In straightforward calculations, $\langle \hat{l}_i^2 \rangle$; $i = x, y, z$ can be easily performed, and hence $\triangle\ \hat{l}_x = \langle \hat{l}_i^2 \rangle - \langle \hat{l}_i \rangle$ is easily obtained. If $\triangle\ \hat{l}_\beta$ satisfies the condition

$$V(\hat{l}_\beta) = \left(\triangle\ \hat{l}_\beta - \sqrt{|\langle \hat{l}_z \rangle|/2} \right) < 0; \qquad \beta = x, y, \tag{60}$$

then the fluctuations in the component $\hat{l}_\beta$ are squeezed, where

$$\triangle\ \hat{l}_\beta = \sqrt{\langle \hat{l}_\beta^2 \rangle - \langle \hat{l}_\beta \rangle^2}, \tag{61}$$

with

$$\langle \hat{l}_x^2 \rangle = \frac{1}{2}[\wp_{ee}(t) + \wp_{eg}(t) + 2\wp_{ii}(t) + \wp_{ge}(t) + \wp_{gg}(t)], \tag{62}$$

$$\langle \hat{l}_y^2 \rangle = \frac{1}{2}[\wp_{ee}(t) - \wp_{eg}(t) + 2\wp_{ii}(t) - \wp_{ge}(t) + \wp_{gg}(t)], \tag{63}$$

$$\langle \hat{l}_z^2 \rangle = [\wp_{ee}(t) + \wp_{gg}(t)]. \tag{64}$$

In view of Eq. (60), we can analyze the periods of squeezing, using the same conditions, as in the previous section. For small values of parameter ξ and ignoring the classical field, the periods of squeezing are alternately formed with respect to $V(\hat{l}_x)$ and $V(\hat{l}_y)$, respectively; see Fig. 4 a. In Fig. 4 b, the squeezing greatly decreases in both $V(\hat{l}_x)$ and $V(\hat{l}_y)$ after increasing of ξ to 20. To activate the role of classical field, we consider $\tau = 0.5$. The periods of squeezing decrease in both $V(\hat{l}_x)$ and $V(\hat{l}_y)$. This result confirms the one obtained from the entropy squeezing by comparison Fig. 3 c and Fig. 4 c. In Fig. 4 d, we show that the squeezing periods completely disappear, when ξ increases, except for some small periods at the beginning of the interaction. In Figs. 4 e, f, one observes confirmation of results previously shown in entropy squeezing – the squeezing periods decrease and the intensity of oscillations increases with increase in the influence of the classical field.

5. The Physical Transient Spectrum

Here, we derive the physical spectrum $S(\nu)$ of the radiation field, which is emitted by the atom in a cavity, calculating the Fourier transform of the time-averaged dipole–dipole correlation function

$$\langle (\wp_{ei}(t_1) + \wp_{eg}(t_1))(\wp_{ie}(t_2) + \wp_{ge}(t_2)) \rangle. \tag{65}$$

The physical spectrum $S(\nu)$ is given by [28, 39]

$$S(\nu) = \Gamma \int_0^T dt_1 \int_0^T dt_2 \exp[-(\Gamma - i\nu)(T - t_1) - (\Gamma + i\nu)(T - t_2)] * \langle (\wp_{ei}(t_1) + \wp_{eg}(t_1))(\wp_{ie}(t_2) + \wp_{ge}(t_2)) \rangle, \tag{66}$$

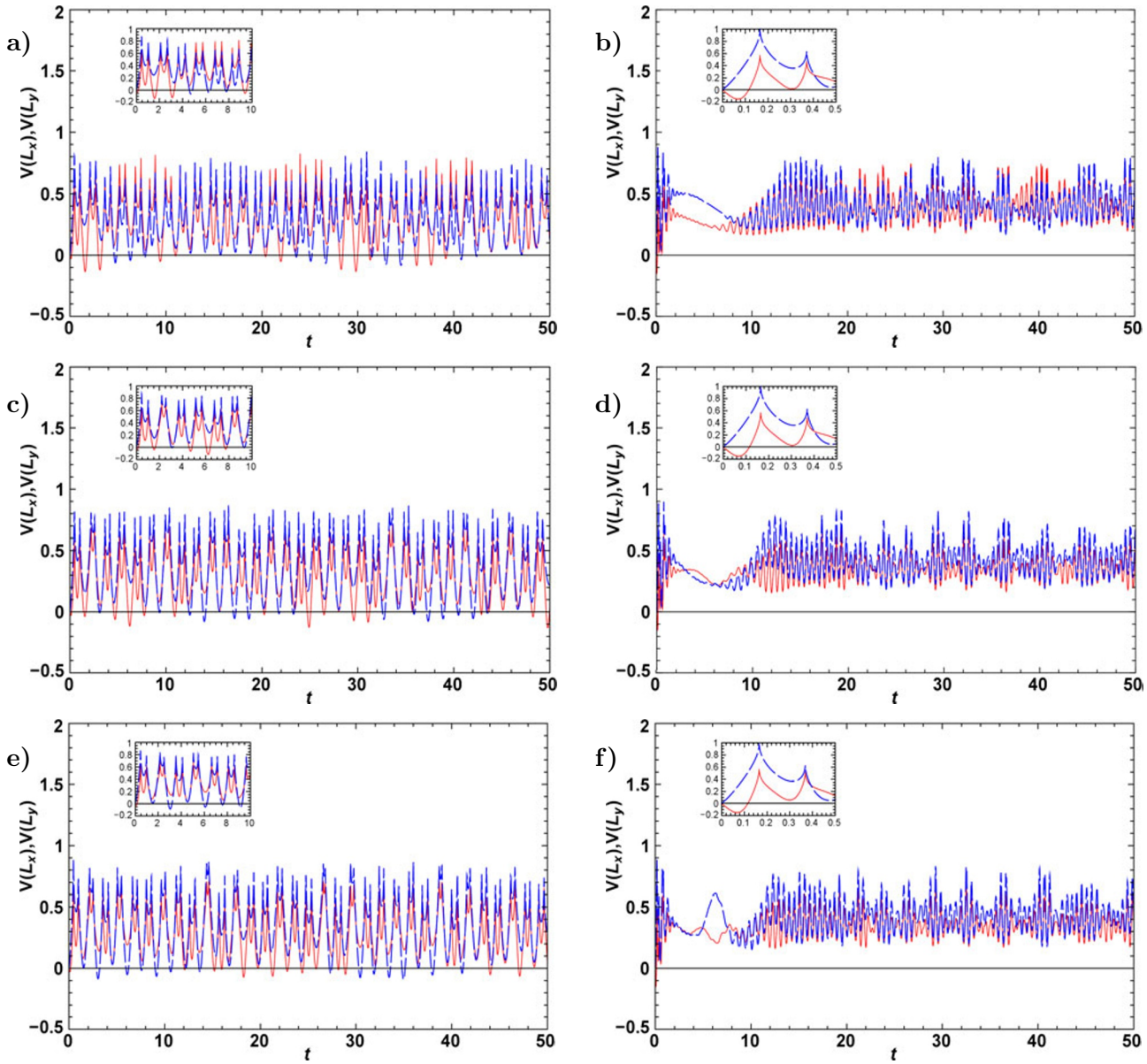

Fig. 4. The time evolution of the variance squeezing components $V(\hat{l}_x)$ (red curves) and $V(\hat{l}_y)$ (blue curves) as functions of scaled time t. The parameters are same as in Fig. 2.

where Γ is the bandwidth of the filter, T represents the interaction time, and ν is the probe field frequency.

After straightforward calculations, we obtain the following expression for the physical emission spec-

trum of the Λ-type three-level atom:

$$
\begin{aligned}
S(\nu) &= |N_q|^2 \sum_{n=0}^{q} \xi^{2n} \frac{(q-n)!}{q!n!} \left\{ \Gamma(\frac{\exp[-2\Gamma T](-1+\exp[TX])(-1+\exp[TX^*])}{|X|^2} \right\} \\
&\times \left\{ (q-n)(n+1) \left(\frac{\Omega^2}{\delta_1^2} + \frac{\Omega^2}{\delta_2^2} + \frac{2\Omega^2}{\delta_1\delta_2} \right) + \frac{\tau^2}{\delta_1^2} + \frac{\tau^2}{\delta_2^2} \right\} \\
&+\Gamma \sum_{n=0}^{q} \left\{ \frac{1-\exp[-T(X^*-i\delta_1)]}{(|X|^2+\delta_1^2)} + \frac{\exp[-T(2\Gamma+i\delta_1)(-\exp[TX^*]+\exp[iT\delta_1])]}{|X^2+\delta_1^2} \right\} \\
&+\Gamma \sum_{n=0}^{q} \left\{ \frac{1-\exp[-T(X^*-i\delta_2)]}{(|X|^2+\delta_2^2)} + \frac{\exp[-T(2\Gamma+i\delta_2)(-\exp[TX^*]+\exp[iT\delta_2])]}{|X|^2+\delta_2^2} \right\} \\
&+\Gamma \frac{\tau}{\delta_1} \left\{ \sum_{n=0}^{q} \left[\frac{\exp[-TX](\exp[-TX^*]-\exp[-iT\delta_2])}{|X|^2-i\delta_2 X} - \frac{\exp[-2\Gamma T](-1+\exp[TX^*])}{|X|^2+i\delta_2 X^*} \right] \right. \\
&\left. + \frac{\exp[-T(X^*-i\delta_2)](-1+\exp[TX^*])}{|X|^2+i\delta_2 X^*} - \frac{\exp[-TX^*]-\exp[-iT\delta_2]}{|X|^2-i\delta_2 X} \right] \Bigg\} \\
&+\Gamma \frac{\tau}{\delta_2} \left\{ \sum_{n=0}^{q} \left[\frac{\exp[-TX](\exp[-TX^*]-\exp[-i\delta_1])}{|X|^2-i\delta_1 X} - \frac{\exp[-2\Gamma T](-1+\exp[TX^*])}{|X|^2+i\delta_1 X^*} \right. \right. \\
&\left. \left. + \frac{\exp[-T(X^*-i\delta_1)](-1+\exp[TX^*])}{|X|^2+i\delta_1 X^*} - \frac{(\exp[-TX^*]-\exp[-iT\delta_1])}{|X|^2-i\delta_1 X^*} \right] \right\}, \qquad (67)
\end{aligned}
$$

where $X = (\Gamma - i\nu)$, $X^* = \Gamma + i\nu$, $\delta_1 = \omega_e - \omega_i$, $\delta_2 = \omega_e - \omega_g$, and $S_j(t_r) = \exp[i\delta_j t_r]$; $j = 1, 2,\ r = 1, 2$.

We analyze the effect of the bandwidth of the filter, the interaction time in addition to the classical field on the emission spectrum, using the conditions $T = 5$, $\Gamma = 0.1$, and $\tau = 0$. In Fig. 5 a, we show the emission spectrum in the resonant case after switching of the classical field. A symmetrical main peak is formed around the vertical axis, and small peaks are formed on both sides of the vertical axis. The maximum value of the main peak at the vertical axis slightly increases after switching of the classical field; see Fig. 5 b. For $T = 0.5$, $\Gamma = 0.01$, and $\tau = 0$, the maximum value of the main peak at the vertical axis significantly decreases compared with the previous case. The maximum values of the small peaks increase on both sides of the vertical axis; see Fig. 5 c. After adding the classical field, the maximum value of the peaks are improved, as obtained previously; see Fig. 5 d.

6. Conclusions

In this paper, we studied the effects of the initial state and the classical field on a system consisting of a three-level atom interacting with a two-mode field. We transformed the atomic system to remove the parts containing the classical field. The constants of motion of the visual system were obtained. Therefore, the solution of the Schrödinger equation was obtained and returned to the wave function that describes the original system. We studied the effects of the initial state and the classical field on a system consisting of a three-level atom interacting with a two-mode field. Our system differs from the one considered in [40], since we used the finite pair coherent state as an initial state of the field but in [40] the field has been prepared in the entangled pair coherent states.

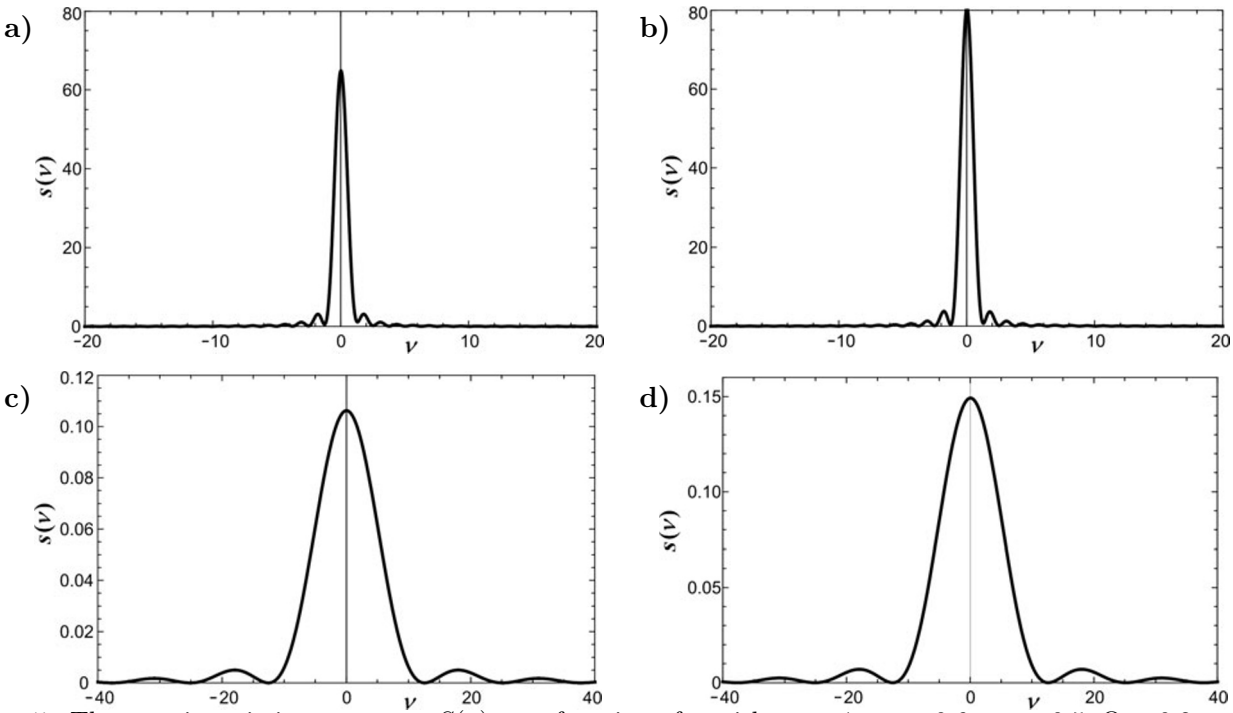

Fig. 5. The atomic emission spectrum $S(\nu)$ as a function of ν with $\omega_e = 1$, $\omega_t = 0.6$, $\omega_0 = 0.5$, $\Omega = 0.2$, $q = 50$, and $\xi = 3$. Here, $T = 5$, $\Gamma = 0.1$, and $\tau = 0$ (a), $T = 5$, $\Gamma = 0.1$, and $\tau = 1$ (b), $T = 0.5$, $\Gamma = 0.01$, and $\tau = 0$ (c), and $T = 0.5$, $\Gamma = 0.01$, and $\tau = 1$ (d).

We investigated the atomic level occupations, entropy squeezing, variance squeezing, and atomic emission spectrum. Our results showed that the initial state of the field was strongly influenced by the level occupations. The occupation oscillates chaotically, when the parameter ξ is small, while the oscillations are regular, when the parameter ξ is large. The occupations of the second and third levels were influenced by the classical field, as they exchanged the loss and gain of energy between them, this phenomenon was also observed in [40]. The squeezing intervals were improved, when the parameter ξ was taken small, while the squeezing intervals decreased, when the parameter ξ was taken large. When the classical field was included, the squeezing intervals were almost erased. For the emission spectrum, a large peak was formed on the vertical axis; moreover, small peaks were formed on either side of the vertical axis. The maximum value increased after adding the classical external field. The maximum values of the peaks decreased after decreasing the influence of both the bandwidth of the filter Γ and the interaction time T.

Acknowledgments

The authors would like to acknowledge Deanship of Scientific Research, Taif University for funding this work.

References

1. S. E. Harris, *Phys. Rev. Lett.*, **62**, 1033 (1989).
2. S. E. Harris, *Phys. Rev. Lett.*, **70**, 552 (1993).
3. J. H. Eberly, M. L. Pons, and H. R. Haq, *Phys. Rev. Lett.*, **72**, 56 (1994).
4. E. M. Khalil, S. Abdel-Khalek, S. Al-Awfi, and M. Rasulova, *J. Intell. Fuzzy Syst.*, **38**, 2817 (2020).
5. E. T. Jaynes and F. W. Cummings, *Proc. IEEE*, **51**, 89 (1963).
6. A. Boca, R. Miller, K. M. Birnbaum, et al., *Phys. Rev. Lett.*, **93**, 233603 (2004).
7. D. Meschede, H. Walther, and G. Müller, *Phys. Rev. Lett.*, **54**, 551 (1985).
8. B. W. Shore and P. L. Knight, *J. Mod. Opt.*, **40**, 1195 (1993).
9. A. M. Abdel-Hafez, A.-S. F. Obada, and M. M. A. Ahmad, *J. Phys. A: Math. Gen.*, **20**, L359 (1987).
10. N. H. Abdel-Wahab, *Phys. Scr.*, **76**, 244 (2007).
11. N. H. Abd El-Wahab, A. S. Abdel Rady, A.-N. A. Osman, and A. Salah, *Middle East J. Sci. Res.*, **23**, 1532 (2015).
12. R. Daneshmand and M. K. Tavassoly, *Eur. Phys. J. D*, **70**, 101 (2016).
13. F. Jahanbakhsh, M. K. Tavassoly, *Mod. Phys. Lett.*, **35**, 2050183 (2020).
14. A.-S. F. Obada, S. Abdel-Khalek, E. M. Khalil, and S. I. Ali, *Phys. Scr.*, **86**, 7 (2012).
15. S. Abdel-Khalek, E. M. Khalil, and S. I. Ali, *Laser Phys.*, **18**, 135 (2008).
16. F. Jahanbakhsh and M. K. Tavassoly, *J. Mod. Opt.*, **68**, 522 (2021).
17. M. S. Abdalla, E. M. Khalil, and A.-S. F. Obada, *Ann. Phys.*, **326**, 2486 (2011).
18. M. S. Abdalla, A.-S. F. Obada, E. M. Khalil, and S. I. Ali, *Laser Phys.*, **23**, 115201 (2013).
19. E. Solano, G. S. Agarwal, and H. Walther, *Phys. Rev. Lett.*, **90**, 027903 (2003).
20. M. Y. Abd-Rabbou, E. M. Khalil, M. M. A. Ahmed and A.-S. F. Obada, *Int. J. Theor. Phys.*, **58**, 4012 (2019).
21. E. M. A. Hilal, S. Alkhateed, S. Abdel-Khalek, et al., *Alex. Eng. J.*, **59**, 1259 (2020).
22. E. M. Khalil, S. Abdel-Khalek, S. Al-Awfi, and M. Rasulova, *J. Intell. Fuzzy Syst.*, **38**, 2817 (2020).
23. A.-B. A. Mohamed, E. M. Khalil, and M. Y. Abd-Rabbou, *Phys. E: Low-Dimens. Syst. Nanostruct.*, **134**, 114839 (2021).
24. C. Hooijer, G.-X. Li, K. Allaart, and D. Lenstra, *Phys. Lett. A*, **263**, 250 (1999).
25. S. Smart and S. Swain, *J. Mod. Opt.*, **41**, 1055 (1994).
26. B. J. Dalton, M. R. Ferguson, and Z. Ficek, *Phys. Rev. A*, **54**, 2379 (1996).
27. B. J. Dalton, M. Bostick, and Z. Fizec, *Phys. Rev. A*, **53**, 4439 (1996).
28. A.-S. F. Obada, A. A. Eied, and G. M. Abd-Al Kader, *J. Phys. B: At. Mol. Opt. Phys.*, **41**, 115501 (2008).
29. A. A. Eied, *Can. J. Phys.*, **93**, 11 (2015).
30. A. A. Eied, *Opt. Spectrosc.*, **120**, 587 (2016).
31. A.-S. F. Obada, N. A. Alshehri, E. M. Khalil, et al., *Results Phys.*, **30**, 104759 (2021).
32. A.-S. F. Obada and E. M. Khalil, *Opt. Commun.*, **260**, 19 (2006).
33. H.-I. Yoo and J. H. Eberly, *Phys. Rep.*, **118**, 239 (1985).
34. J. von Neumann, *Mathematical Fundations of Quantum Mechanics*, Princeton University Press (1955).
35. J. S.-Ruiz, *Phys. Lett. A*, **201**, 125 (1995).
36. J. S.-Ruiz, *Phys. Lett. A*, **226**, 7 (1997).
37. C.-Y. Zhang and M.-F. Fang, *Chin. Phys. B*, **30**, 010303 (2021).
38. A.-S. F. Obada, M. M. A. Ahmed, M. Abu-Shady, et al., *Phys. Scr.*, **96**, 045105 (2021).
39. G. S. Agarwal, R. K. Bullough, and N. Nayak, *Opt. Commun.*, **85**, 2020 (1991).
40. A.-S. F. Obada, E. M. Khalil, S. Sanad, and H. F. Habeba, *Int. J. Opt.*, **2022**, 1 (2022).